Published in final edited form as:
Immunity. 2013 October 17; 39(4): 711–721. doi:10.1016/j.immuni.2013.09.004.

Processing of human Toll-like receptor 7 by furin-like proprotein convertases is required for its accumulation and activity in endosomes

Madeleine M. Hipp[1], **Dawn Shepherd**[1], **Uzi Gileadi**[1], **Michael C. Aichinger**[1], **Benedikt M. Kessler**[3], **Mariola J. Edelmann**[3], **Rachid Essalmani**[4], **Nabil G. Seidah**[4], **Caetano Reis e Sousa**[2,#], and **Vincenzo Cerundolo**[1,#]

[1]MRC Human Immunology Unit, Weatherall Institute of Molecular Medicine, University of Oxford, Oxford OX3 9DU, UK

[2]Immunobiology Laboratory, Cancer Research UK, London Research Institute, London WC2A 3PX, UK

[3]Henry Wellcome Building for Molecular Physiology, Nuffield Department of Medicine, Wellcome Trust Gene Centre, Churchill Hospital, Oxford, OX3 7BN, UK

[4]Institut de Recherches Cliniques de Montréal (IRCM), affiliated to the University of Montreal, Montréal, Québec H2W 1R7, Canada

Summary

Toll-like receptor 7 (TLR7) triggers antiviral immune responses by recognizing viral single-stranded RNA in endosomes but the biosynthetic pathway of human TLR7 (hTLR7) remains unclear. Here, we show that hTLR7 is proteolytically processed and that the C-terminal fragment selectively accumulates in endocytic compartments. hTLR7 processing occurred at neutral pH and was dependent on furin-like proprotein convertases (PCs). Furthermore, TLR7 processing was required for its functional response to TLR7 agonists such as R837 or influenza virus. Notably, pro-inflammatory and differentiation stimuli increased the expression of furin-like PCs in immune cells, suggesting a positive feedback mechanism for TLR7 processing during infection. As self RNA can under certain conditions activate TLR7 and trigger autoimmunity, our results identify furin-like PCs as a possible target to attenuate TLR7-dependent autoimmunity and other immune pathologies.

Keywords

Toll-like receptor 7; Furin-like proprotein convertases; Plasmacytoid dendritic cells; Cathepsins; Autoimmunity

Corresponding authors: vincenzo.cerundolo@imm.ox.ac.uk, phone: +44 (0) 1865 222412, Fax: +44 (0)1865 222502, caetano@cancer.org.uk, phone: +44 (0) 20 7269 2832, Fax +44 (0)20 7269 3479.
[#]C.R.S and V.C. share last authorship for this work.

Europe PMC Funders Author Manuscripts

Introduction

Toll-like receptors (TLRs) have emerged as major regulators of innate and adaptive immune responses to infection. Many TLRs recognize products of microbial biosynthesis pathways, which are absent in mammals, allowing for qualitative discrimination between microbial and host cells (Akira et al., 2006). In contrast, TLR7 and 8 respond to viral and bacterial single stranded (ss) RNA and TLR9 to DNA which, barring small differences, are effectively invariant between host and pathogen. This raises the issue of how TLRs 7, 8 and 9 can successfully discriminate self from nonself. The nucleic acid-recognizing TLRs do not respond to their ligands at the cell surface but in endosomes (Blasius and Beutler, 2010; Kagan, 2012). This has led to the notion that discrimination is achieved on the basis of ligand localization and that responses to self nucleic acids are avoided in part through the absence of the latter from endosomal compartments (Blasius and Beutler, 2010; Kagan, 2012). Consistent with that notion, TLR7 and 9 can respond to self RNA or DNA, respectively, if the latter are deliberately introduced into the endocytic pathway (Diebold et al., 2004; Diebold et al., 2006; Heil et al., 2004; Leadbetter et al., 2002). This process may occur naturally in some instances and contribute to autoimmunity in genetically-susceptible individuals (Krug, 2008; Shlomchik, 2009).

Newly synthesized TLR7, 8 and 9 translocate into the endoplasmic reticulum (ER), from which they traffic to endosomes with help of the associated protein, Unc93B1 (Brinkmann et al., 2007; Kim et al., 2008; Lee et al., 2013). A possible explanation as to why nucleic acid-recognizing TLRs only respond to their ligands within endosomal compartments has come from the observation that they undergo proteolytic cleavage in endosomes and that this cleavage is necessary for receptor activity (Ewald et al., 2011; Lee et al., 2013; Park et al., 2008; Sepulveda et al., 2009). Low pH-dependent endosomal cathepsins, as well as asparaginyl endopeptidase (AEP), process mouse TLR (mTLR)9 and these proteases might constitute attractive targets for inhibition in cases of TLR-driven autoimmunity or pathological inflammation (Ewald et al., 2011; Park et al., 2008; Sepulveda et al., 2009). mTLR7 is also cleaved by AEP (Maschalidi et al., 2012). However, inhibition of cathepsins or AEP does not completely prevent mouse TLR processing (Ewald et al., 2008; Sepulveda et al., 2009), indicating involvement of additional proteases. In addition, although human TLR (hTLR)9 has also been suggested to be cleaved by AEP (Sepulveda et al., 2009), most analysis of TLR processing has been carried out with the mouse receptors. Thus, there is a need to establish if all TLRs are processed similarly, whether this is true for human as well as mouse receptors and what other proteases might be involved in cleavage.

The furin-like proprotein convertases (PCs) are a family of proteases involved in processing of many polypeptides (Seidah et al., 2008), including Notch, viral glycoproteins, growth factors and their receptors, neuropeptides, metalloproteases, adhesion molecules, enzymes, and even toxins (Hallenberger et al., 1992; Logeat et al., 1998; Molloy et al., 1992; Rousselet et al., 2011b; Zarkik et al., 1997). Furin-like PCs encompass a family of nine calcium-dependent serine endoproteases of the subtilisin-kexin type called PC1/3, PC2, Furin, PC4, PC5/6, PACE4, PC7, SKI-1/S1P, and PCSK9 (Seidah et al., 2008). The first seven enzymes cleave their substrates after the C-terminal residue at sites bearing the consensus motif matching the consensus $K/Rx_nK/R$, where x indicates any amino acid

residue, K/R designates a lysine or an arginine residue, and n is 0, 2, 4, or 6 (Seidah et al., 2008). PCs are synthesized as inactive proenzymes and the inhibitory prosegment is removed through an initial autocatalytic processing event in the ER (all but PC2) or in immature secretory granules (PC2) (Fugere et al., 2002; Seidah et al., 2008). The heterodimer complex, consisting of the inhibitory prosegment and the rest of the molecule, then traffics from the ER to specific subcellular compartments where catalytic activity is acquired, usually after a second autocatalytic cleavage of the prosegment that results in its release from the active enzyme (Seidah et al., 2008). PC1/3 and PC2 are restricted to dense core secretory granules of secretory cells while PC4 is found primarily in testicular and ovarian tissues. In contrast, furin, PACE4, PC5/6A, PC5/6B, and PC7 are ubiquitously expressed in multiple cell types and located throughout the secretory pathway (Fugere et al., 2002; Seidah et al., 2008). Notably, PCs can be active at neutral pH (Decroly et al., 1996; Malfait et al., 2008; Molloy et al., 1992) and generally cleave their substrates in the trans-Golgi network (TGN), elsewhere along the secretory pathway or at the cell surface (Rousselet et al., 2011a; Seidah et al., 2008). Rarely, cleavage can also occur in early biosynthetic compartments such as the ER in cases where the substrate outcompetes the inhibitory prosegment of the convertase (Salvas et al., 2005). Their broad expression pattern, cleavage specificity, ability to act in endosomes and localization along the secretory pathway suggest that some furin-like PCs could potentially contribute to TLR processing.

In this study, we show that hTLR7 undergoes proteolytic processing and that the C-terminal fragment of the receptor selectively accumulates in endocytic compartments. hTLR7 processing was independent of low pH and largely independent of cathepsin activity. Instead hTLR7 processing was dependent on the action of furin-like PCs. Our data underscore the notion that endosomal TLRs are regulated by proteolysis and indicate that this can occur at neutral pH, possibly in early endosomes or in a pre-endosomal compartment, such as the ER, Golgi, plasma membrane. These results have implications for our understanding of self/nonself nucleic acid discrimination and highlight furin-like PCs as a possible target in attenuation of TLR7-dependent autoimmunity and other immune pathologies.

Results

Processing of Human TLR7 Generates a Truncated C-terminal Fragment that Accumulates in Phagosomes

To determine whether hTLR7 undergoes post-translational proteolytic processing, we tagged hTLR7 with a hemagglutinin (HA) epitope at the carboxyl (C) terminus (TLR7-HA) and stably expressed it in THP-1 (THP-TLR7), HEK293null (293null-TLR7) and LoVo (LoVo-TLR7) cell lines. Western blot analysis with anti-HA revealed a prominent band corresponding to the expected ~150 kD polypeptide, which was absent from green fluorescence protein (GFP)-expressing controls (Figure 1A). Notably, anti-HA additionally detected a fainter band at around ~75 kD in TLR7-HA-expressing cells, but not in GFP-expressing controls (Figure 1A). We confirmed that the 75 kD polypeptide corresponds to a C-terminal fragment of TLR7 by immunoprecipitation from lysates of THP-TLR7 followed by SDS-PAGE and mass spectrometry analysis of the excised band (Figure 1B). Figure 1C shows the protein sequence of hTLR7 with the peptides detected by mass spectrometry

highlighted in black. All peptides mapped C-terminal of a region encompassing residues 455–493 (Figure 1C, blue). This region is thought to form a flexible loop between the leucine-rich repeats (LRR) 14 and 15 (Bell et al., 2003) and its exposure might therefore make it a suitable target for proteolytic enzymes.

Pre-treatment of THP-TLR7 cells with PMA to induce differentiation into macrophage-like cells, or with pro-inflammatory cytokines such as IFN-γ or IFN-α, led to an increase in total detectable amount of TLR7 (Figure S1A, B, and data not shown). The same treatments also increased the ratio of truncated 75 kDa to full-length 150 kDa TLR7 (Figure 2A, B and Figure S1A, B) and potentiated the ability of THP-TLR7 cells to produce IL-8, IL-6, and TNF-α in response to the specific TLR7 agonist, R837 (Figure 2A and B and data not shown). Increased detection of truncated TLR7 was also seen after treatment with the TLR4 agonist LPS (Figure 2C). Similarly, pretreatment of primary human B cells with PMA, B cell receptor crosslinking ± CD40L, IFN-α or IFN-γ also enhanced their ability to respond to R837, as measured by cell surface staining for CD83 (Figure S1C and data not shown). Thus, exposure of cells to differentiation-inducing or pro-inflammatory cytokines increases the amount of truncated TLR7 in total cell lysates and/or responsiveness to TLR7 agonists.

We investigated whether truncated TLR7 might correspond to a signaling competent form of the receptor that localizes selectively to the endocytic pathway, in which ligand is encountered. Consistent with that notion, phagosome preparations isolated from R837-stimulated THP-TLR7 that had been fed latex beads contained almost exclusively truncated TLR7 (Figure 2D). This was in contrast to cell lysates, which contained the usual ratio of truncated and total receptor (Figure 2D). As expected, phagosome preparations were positive for the lysosomal protein LAMP1 but devoid of the ER marker calnexin (Figure 2D). Cleaved TLR7 was detected in phagosomes isolated as early as 15 min after latex beads incubation and cleavage was unaffected by the addition of R837 (Figure S1D and E). We conclude that hTLR7, like mTLR9 (Ewald et al., 2008) and mTLR7 (Maschalidi et al., 2012), undergoes N-terminal processing to generate a C-terminal fragment that selectively accumulates in endocytic compartments.

Human TLR7 Processing is Independent of Low pH

Processing of mTLR7 and 9 mediated by cathepsins of the cysteine protease family and/or AEP is strictly dependent on endosomal acidification (Ewald et al., 2008; Park et al., 2008; Sepulveda et al., 2009). We examined the effect of raising endosomal pH in THP-TLR7 cells that had been pre-treated with PMA to increase generation of truncated receptor (see above). The ratio of truncated to total TLR7 in total cell lysates, as well as the appearance of truncated TLR7 in phagosomes, was unaffected by bafilomycin A, an inhibitor of the vacuolar H^+-ATPase, or monensin, a monovalent ionophore that dissipates proton gradients (Figure 3A). As a positive control, the same drug treatments blocked the conversion of pro-cathepsin (Cat)B into mature enzyme and the trafficking of mature CatB into phagosomes, as detected by probing cell lysates and phagosomal fractions, respectively (Figure 3A). However, the block in acidification prevented IL-8 production by PMA-treated THP-TLR7 cells in response to R837 without affecting the viability of the cells or their response to LPS (Figure S2A). Furthermore, when we used the broad range cathepsin inhibitor E64

supplemented with inhibitors specific for CatS and CatK, we did not see inhibition of either TLR7 processing or R837-elicited IL-8 production (Figure 3B, C). However, when we used EST, a more cell permeable version of E64, we saw accumulation of full-length TLR7 alongside cleaved TLR7 in phagosomes (Figure 3B). Nevertheless, EST was not sufficient to decrease the functional response of THP-TLR7 cells to R837 (Figure 3C, right panel). Thus, endosomal acidification and cathepsin-like activity appear largely dispensable for processing of hTLR7 in THP-1 cells.

Calcium Dependent Serine-Proteases of the Furin-like PCs Mediate Processing of Human TLR7

To test the involvement of other proteases in TLR7 processing, PMA differentiated THP-TLR7 were treated with a range of inhibitors. To obviate possible toxicity and to control for specificity, we first titrated all drugs to identify the maximum concentration that did not cause cell death or prevent responses to LPS (Figure S2B and data not shown). The serine-protease inhibitor AEBSF reduced the detection of truncated TLR7 in cell lysates and decreased the response of THP-TLR7 to R837, but not LPS when compared to the DMSO control (Figure 4A). Similar results were obtained with a second serine protease inhibitor, TPCK (data not shown). In addition, calcium depletion using EDTA in combination with the calcium ionophore A23187 also reduced cleavage of TLR7 and selectively impaired the response of THP-TLR7 to R837, but not to LPS (Figure 4B). Taken together, these results suggested the involvement of a calcium-dependent serine protease in hTLR7 processing.

THP-1 cells contained mRNA for furin, PC1/3, PACE4, PC5/6, and PC7, especially after PMA-induced differentiation or treatment with pro-inflammatory cytokines (Figure S3A and data not shown). We confirmed by Western blot that PMA, LPS and IFN-γ induce the upregulation of furin protein in THP-1 cells (Figure S3B). Therefore, we tested whether TLR7 processing in PMA-treated THP-TLR7 cells was affected by DC1, a dicoumarol derivative that potently inhibits furin, PACE4, PC5/6 and, to a lesser extent, PC7 (Komiyama et al., 2009). Notably, DC1 treatment reduced the ratio of truncated to total TLR7 in total lysates of THP-TLR7 cells, which correlated with a decrease in the response to R837, but not to LPS (Figure 4C). The loss of TLR7 processing was more marked when phagosomal fractions were examined: as shown in Figure 4D, DC1 pre-treatment led to a complete loss of truncated TLR7 from THP-TLR7 phagosomes, which, instead now contained full-length receptor. Similar results were obtained with DC2, another dicoumarol derivative that preferentially inhibits PC7 but has an additional effect on furin, PACE4 and PC5/6 (data not shown) (Komiyama et al., 2009).

LoVo cells do not produce functional furin (Takahashi et al., 1993; Zarkik et al., 1997) but express mRNA for PACE4, PC5/6 and PC7 (data not shown). Like THP-TLR7 cells, LoVo cells expressing TLR7 (but not parental LoVo) were able to respond to R848 (another TLR7 agonist; Fig. 5B and data not shown). Thus, our data suggest that other members of the furin-like PC family can substitute for furin in promoting TLR7 cleavage. To assess the role of PC5/6 and PC7 in TLR7 processing, we generated LoVo-TLR7 cells stably expressing the preprosegments of PC5/6 (ppPC5) and/or PC7 (ppPC7), which act as specific inhibitors of the respective mature PC (Figure 5A) (Fugere et al., 2002; Nour et al., 2003; Zhong et al.,

1999). Expression of either ppPC5 or ppPC7 or, in particular, both preprosegments, led to a marked reduction in R848-induced IL-8 secretion (Figure 5B) and TLR7 processing (Figure 5C and data not shown). Thus, both proteases appear to process hTLR7. We then decreased PC5, PC7 or furin expression in THP-TLR7 using shRNA lentiviral particles targeting the respective proteases. Furin knockdown resulted in marked inhibition of TLR7 processing and of IL-8 production in response to R837 but not LPS (Figure 5D). This effect was seen with 5 different individual shRNA constructs targeting different regions of furin, used separately or in combination (Figure 5D and data not shown). Consistent with these data, we were able to show furin in phagosomes of THP-1 cells (Figure S1E and data not shown). Knockdown of PC7, but not PC5, also inhibited TLR7 processing and R837 responsiveness to some degree (data not shown). We conclude that furin-like PCs in THP-1 and LoVo cells are necessary for processing of hTLR7.

Mutation of a Potential PC Recognition Site Reduces Human TLR7 Processing and Signalling

The hTLR7 protein sequence contains a prominent cluster of five putative PC cleavage sites between residues 467 and 480 within the flexible loop between LRR 14 and 15 (Figure 1C and Figure S4A). To further examine the role of furin-like PCs in the processing of full length TLR7, we removed all of the predicted furin-like PC recognition sites within the undefined region by replacing arginine 467 and arginine 473 with alanines (TLR7-mut; Figure 5E and Figure S4A). Normal amounts of the TLR7-mut were expressed in PMA-differentiated THP-1 cells but the fraction of truncated protein was reduced (Figure 5F). This correlated with a lower response to R837 when compared to cells bearing wild type TLR7 (Figure 5F), while the response to LPS was unaffected (Figure S4B). TLR7-mut was able to traffic to late endosomes and the extent of co-localization with the endosomal marker Lamp1 was similar for TLR7 and TLR7-mut (Figure S4C, D). We conclude that abrogation of putative furin-like PC cleavage sites in the flexible loop between LRRs 14 and 15 impairs processing of hTLR7 and decreases generation of a signalling-competent TLR7.

The C-terminal Portion of Human TLR7 is Signalling-competent

To verify the truncation site identified by site directed mutagenesis and mass spectrometry analysis of the cleaved C-terminal fragment, we made HA-tagged hTLR7 C-terminal fragments (Cterm) of different lengths, starting after the different possible cleavage sites within the undefined region (Figure S5A). The construct CtermK starts at amino acid 481 and ends at position 1049, and therefore is similar to the C-terminal fragment of mTLR7, ranging from residue 480 to 1052, that is functionally active in cells over-expressing Unc93B1 (Maschalidi et al., 2012). We expressed all constructs in THP-1 cells (THP-Cterm) and carried out Western blot analysis of PNGase F treated cell lysates to eliminate the confounding effects of glycosylation (Figure S5B). The truncated version naturally found in cells expressing wild type TLR7 ran at an apparent molecular weight between those of constructs CtermH to K (Figure S5B). Therefore hTLR7 processing occurs at one of the potential furin-like PC recognition sites between amino acids 470 and 480.

Surprisingly, none of the C-terminal fragments rendered THP-1 cells responsive to R837 (Figure 6A and data not shown). This was not due to a lack of Unc93B1, as all transfectants

expressed amounts of endogenous Unc93B1 (Figure S5C top panel and data not shown) comparable to those in cell lysates of primary peripheral blood mononuclear cells (PBMCs), plasmacytoid dendritic cells (pDCs) and B cells (Figure S5C bottom panel). Nevertheless, overexpression of C-terminally FLAG-tagged Unc93B1 (Figure S5D) did increase the IL-8 response of THP-CtermK cells to R837 by around 10-fold (Figure 6A) and revealed the functional activity of the CtermK fragment, albeit at lower activity than for full length TLR7 (Figure 6A).

An explanation for the reduced ability of the TLR7 C-terminal fragment to restore completely IL-8 response to R837 could be that the TLR7 N-terminal fragment is required to ensure efficient TLR7 trafficking into the endo-lysosomal compartment. Consistent with that notion, the CtermK fragment was not detected in phagosome fractions even though it could be easily detected in the pre-gradient controls (Figure S5E). We hypothesized that full length TLR7 might be able to form a heterodimer with CtermK and escort the latter to the endocytic pathway. To test this hypothesis, THP-1 cells expressing the CtermK fragment and the full length TLR7 were tested for their ability to respond to R837 in the presence or absence of DC1, which inhibits the biological activity of full length TLR7 but should not affect that of the CtermK fragment. Consistent with this prediction, THP-1 cells co-expressing full length TLR7 and the CtermK fragment produced IL-8 in response to R837 and were resistant to DC1 inhibition (Figure S5F). In contrast, as before, DC1-treated THP-1 cells expressing full length TLR7 alone failed to respond to R837 stimulation (Figure S5F). Thus, expression of full-length TLR7 partially restores the activity of CtermK fragment in trans. Consistent with these findings, preliminary observations suggest that overexpression of the N-terminal hTLR7 fragment can also partially restore the functional activity of the C-terminal fragment (data not shown).

Finally, we extended these results by examining coupling to the downstream signalling adaptor, MyD88. Confocal microscopy analysis showed that R837 stimulation enhanced co-localization of MyD88 with TLR7 in THP-TLR7 cells treated with DMSO, but not in cells treated with DC1 (Figure 6B and C). As phagosomes purified from untreated THP-TLR7 cells only contain cleaved TLR7, while those purified from DC1-treated cells contain the full-length TLR7 (Figure 2D and Figure 4D), these data indicate that MyD88 is specifically recruited in a ligand-dependent manner to endosomes containing the TLR7 C-terminal fragment but not full-length TLR7.

Furin-like PCs are Required for TLR7 Responsiveness in Primary Human pDCs and B cells

In humans, TLR7 expression is predominantly found on pDC and B cells. We purified human pDCs from peripheral blood by positive selection and cultured them with DC1 inhibitor or with solvent alone (DMSO). Unfortunately, the lack of antibodies suitable for biochemical detection of TLR7 prevented assessment of endogenous TLR7 cleavage in primary cells (data not shown). Nevertheless, across multiple experiments with cells from different donors, we noticed that pDCs pre-incubated with DC1 secreted markedly less IFN-α in response to R837 or heat-inactivated (56 °C for 30 min) influenza virus (hiFlu), another TLR7 agonist (Diebold et al., 2004), when compared to DMSO-treated cells (Figure 7A). In addition, cathepsin inhibitors had little effect on the response to hiFlu, even though they

decreased the response to R837 (Figure S6A). We ruled out that lack of IFN-α was due to a toxic effect of the inhibitors by monitoring cell viability (data not shown) and metabolic activity (Figure S6B). As an additional source of cells expressing endogenous amounts of TLR7, we generated human IFN-DCs from blood monocytes by differentiation in the presence of IFN-α and GM-CSF (Mohty et al., 2003). Treatment of these cells with DC1, but not with DMSO, reduced their ability to produce IL-8 in response to R837 but not to LPS (Figure 7B), without affecting cell viability (data not shown). DC1 treatment of B cells isolated from peripheral blood decreased IL-8 secretion and upregulation of CD80 in response to R837 or hiFlu (Figure 7C). In contrast, the same response was not decreased by EST (data not shown). Next, we assessed the effect of furin-like PC inhibitors on the functional response to TLR9 agonists, as the lack of suitable antibodies prevented direct assessment of TLR9 cleavage. As shown in Figure 7D and E, DC1 markedly reduced CpG-induced activation of human pDCs and B cells. In contrast, cathepsin inhibitors had no effect on pDCs in the same assay (Figure S6A, right panel). None of the inhibitors was toxic to the cells (Figure S6B).

PMA treatment enhanced expression of furin protein in pDCs, IFN-DCs, PBMCs and B cells (Figure S6C). In pDCs furin was also upregulated by IFN-α treatment (Figure S6C) and in B cells by engagement of the B cell receptor, especially in combination with CD40L (Figure S6C). Furthermore, B cell receptor crosslinking, IFN-γ and IFN-α all increased furin, PC5 and PC7 transcripts in B cells (Figure S6D). We conclude that furin-like PC activity is required to generate signalling-competent TLR7 in primary human cells and that expression of furin-like PCs is increased in those cells by exposure to pro-inflammatory and differentiation inducing stimuli.

Finally, we assessed whether the role of furin-like PCs in TLR processing might extend to mouse. The aligned mouse and human TLR7 sequences showed (Figure 1C, bottom panel) furin-like PC recognition sites at the exact same positions. DC1 treatment reduced secretion of IL-12p40 by mouse macrophages in response to R837 and CpG but not LPS (Figure S6E). However, consistent with previously published data (Ewald et al., 2008; Maschalidi et al., 2012), in mouse macrophages cathepsin inhibition also strongly decreased responses to TLR7 and 9 agonists (data not shown). Thus, furin-like PCs play a role in the processing of TLRs across cell types and species, but other families of proteases also contribute to differing degrees.

Discussion

The recent finding that endosomal TLRs require processing by low pH-dependent proteases has gained much attention as a mechanism for reinforcing self/nonself nucleic acid discrimination. However, most studies supporting this concept have been carried out with mTLR9 (Ewald et al., 2008; Park et al., 2008; Sepulveda et al., 2009) or, more recently, mTLR7 (Maschalidi et al., 2012) and have not been extended to human TLRs. In this study, we show that hTLR7 is proteolytically cleaved in different human immune and nonimmune cells and that receptor processing is required for functional activity. Notably, TLR7 cleavage generates a C-terminal fragment that selectively accumulates in compartments of the endocytic pathway and yet the processing event is independent of the low pH found in those

compartments, making the involvement of acidic proteases unlikely. Although our data do not fully rule out the involvement of cathepsins, in particular ones that might be active at neutral pH, we show that TLR7 processing requires calcium-dependent serine proteases of the furin-like PC family and identify an important site of furin-like PC cleavage within the loop between LRRs 14 and 15. These data extend to hTLR7 the processing paradigm first established for mTLRs, but unexpectedly reveal that it can occur independently of endosomal acidification and highlight furin-like PCs as an important family of proteases in the regulation of innate immune recognition.

Because acidification does not appear required for hTLR7 cleavage, processing can occur before the receptor reaches late endosomes, consistent with the fact that PCs can exert catalytic activity throughout the biosynthetic pathway. Thus, TLR7 cleavage might occur as early as the ER or Golgi before diversion of the receptor to the endocytic pathway (Lee et al., 2013). This early cleavage would ensure that a signaling competent form of the receptor is already present in early endosomal compartments with low cathepsin content where TLR7 signaling has been reported to initiate (Honda et al., 2005a; Honda et al., 2005b; Sasai et al., 2010). However, our data also suggest that the N-terminus of TLR7 helps direct the receptor to the appropriate endosomal compartment, in which case its premature loss would be detrimental. A recent study indicates that C- and N-terminal fragments of mTLR7 can remain linked to each other via disulfide bonds after cleavage (Kanno et al., 2013). Thus, early TLR7 cleavage by furin-like PCs need not preclude N-terminal-directed trafficking to endosomes in the absence of disulfide reduction. Although acidification was dispensable for cleavage, it remained necessary for cellular responses to TLR7 agonists. The question why low pH is important for ligand recognition and signaling by endosomal TLRs remains unresolved (Rutz et al., 2004), but may be related to the protonation of specific histidine residues at acidic pHs within the ligand binding domain of TLRs (Govindaraj et al., 2011; Pirher et al., 2008). Another possibility is that low pH-dependent thiol reductases facilitate reduction of a putative disulfide link between the pre-cleaved N- and C-terminal fragments and release of the signaling-competent TLR C-terminal fragment in the appropriate endosomal compartment.

Several of our findings were obtained using transfected cells overexpressing TLR7 in which some components of the TLR biosynthetic pathway might be limiting. This was not the fact for the more obvious player, Unc93b1 (Kim et al., 2008; Tabeta et al., 2006), as overexpression in THP-TLR7 enhanced the functional response to TLR7 agonists only slightly. Furthermore, we validated our results using IFN-α differentiated monocyte-derived DCs and human blood pDCs and B cells. Inhibition of furin-like PCs but not cathepsins in these cells resulted in a reduced functional response to agonists of TLR7 and also of TLR9, arguing that our conclusions are generally applicable to TLR7 and, possibly, also to TLR9 regulation in primary human cells. Whether they are also applicable to the other nucleic acid sensing TLRs, such as TLR3 or 8, remains to be investigated. We also found that treatment of human primary B cells or THP-TLR7 cells with TLR7 agonists resulted only in a weak response, which could be markedly potentiated by pre-treating with pro-inflammatory and differentiation stimuli. Those stimuli greatly increased the expression of furin-like PCs and enhanced TLR7 processing. Enhanced processing of TLR7 induced by inflammatory stimuli may therefore serve as a positive feedback mechanism during infection. In contrast, in non-

inflammatory situations, TLR7 processing might be limiting, contributing to preventing TLR7 activation by self-RNA reaching endosomal-lysosomal compartments.

Our preliminary studies suggest that furin-like PCs may also play a role in generating functional mTLR7 and 9 in mouse macrophages. On the other hand, cathepsins and AEP clearly have a dominant role in processing of mTLRs (Ewald et al., 2008; Maschalidi et al., 2012; Park et al., 2008; Sepulveda et al., 2009). Such results suggest that TLR7 cleavage may be differentially regulated in human versus mouse, as well as in different cell types. Differential protease dependence may also apply to different activation states of the same cell. Thus, it may be possible to envisage strategies that selectively inhibit TLR processing in specific cells by targeting different classes of proteases. In this regard, derivatives of dicoumarol have been extensively used in the clinic as anticoagulants and show high bioavailability and relatively low toxicity (Benjamin, 1962). Our finding that furin-like PCs play an important role in TLR7 processing in human pDCs suggests that selective inhibition of PCs by dicoumarol derivatives could be useful as a therapeutic approach for TLR7- and pDC-driven immune pathologies, such as systemic lupus erythematosus.

Experimental Procedures

More detailed description of reagents and experiments can be found in the Supplemental Information.

Generation of IFN-DCs, and pDC and B Cell Isolation

Human IFN-DCs were generated by *in vitro* differentiation of the $CD14^+$ subpopulation of PBMCs as described previously (Mohty et al., 2003). BDCA-4^+ pDCs and $CD19^+$ B cells were MACS sorted from leucocytes according to the manufacturer's instruction.

DNA Cloning, Site-directed Mutagenesis, Lentiviral Transduction, and Gene Knockdown

hTLR7 tagged at the C-terminus with HA was cloned into the lentiviral vector pHR-SIN-IRES-Em (Demaison et al., 2002). Double mutations were inserted using the quick QuikChange II XL Site-Directed Mutagenesis Kit (Stratagene) according to the manufacturer's conditions. MISSION shRNA lentiviral vectors were from Sigma-Aldrich. Lentiviral vectors encoding FLAG-tagged Unc93B1 or MyD88 were from GeneCopoeia. Cells transduces with lentiviruses were selected by FACS sorting or puromycin selection.

Cell Lysis and Quantitative Immunoblot Analysis

10^6 cells were lysed in 50 μl 1% (v/v) Triton X-100 based lysis buffer. Where indicated, samples were digested with PNGAse F (NEB). Proteins were separated by SDS-PAGE and standard Western Blot analysis was performed. To calculate the percentage of truncated TLR7 per lane, the intensity of the band of processed TLR7 was divided by the intensity of the band of total TLR7 (shorter + longer fragment).

Large-scale Immunoprecipitation and Tandem Mass Spectrometry

Lysate of PMA-differentiated THP-TLR7 cells was pre-cleared with mouse IgG-Agarose (Sigma), and immunoprecipitated using anti-HA-Agarose Clone HA-7 (Sigma). Eluted

polypeptides were visualized by silver staining on SDS-PAGE, and then tandem mass spectrometry was performed on bands of interest.

IL-8, IFN-α and mIL12-p40 Assay

Cells were stimulated for 24 hrs with indicated TLR agonists. Conditioned medium was collected and secretion of hIL-8, hIFN-α or mIL-12p40 was analyzed by enzyme-linked immunosorbent assay (ELISA).

Phagosome Isolation

Latex beads were fed to PMA differentiated THP-1 cells, and cells were then disrupted by dounce homogenization. Latex-bead-containing phagosomes were isolated on a 60-10% sucrose step gradient after ultracentrifugation. Phagosomes were lysed in lysis buffer, and proteins were separated by SDS-PAGE and visualized by immunoblot.

Transient Transfection and Antibiotic Selection

LoVo cells (70-90 % confluence) were transiently transfected by mixing either 1 or 2 μg each of cDNAs of ppPC5 (Nie et al., 2003), or ppPC7 (Zhong et al., 1999) with 6 μl FuGENE-6 as described by the manufacturer. After 12 hrs successfully transfected cells were selected by adding G418.

Confocal microscopy

PMA differentiated THP-1 cells were fixed, permeabilized with 0.5 % Triton-X 100, blocked, and then stained with primary followed by secondary antibodies. Images were taken using a confocal microscope and Li´s coefficient was calculated to measure the extend of co-localization.

Semi-quantitative RT-PCR

Semi-quantitative RT-PCR for amplification of ppPC5 and ppPC7, and for GAPDH as housekeeping gene was performed as described in the Supplemental Information.

Statistics

All values are represented as the mean ± S.D. An unpaired two-way Student's t test was performed to determine difference between the control and treated group. Significance was accepted at $p < 0.05$ versus control. *, $p < 0.05$; **, $p < 0.01$; ***, $p < 0.001$; ****, $p < 0.0001$.

Supplementary Material

Refer to Web version on PubMed Central for supplementary material.

Acknowledgements

The authors thank Carmela De Santo for generous practical and advisory input, Sarah Booth, Giorgio Napolitani for advisory input, and Moira Johnson for critical reading and editing of the manuscript. We thank Graeme Ball (Micron Oxford, Advanced Bioimaging Unit) for helping with the Fiji analysis, and Laurence Chaperot as well as Joël Plumas (Université Joseph Fourier, Grenoble, France) for experimental help. This work was supported by the

Medical Research Council, UK, CRUK (Programme Grant # C399/A2291 to VC and LRI core support to CRS), DC-THERA, European Commission Sixth Framework Programme (Project Number 512074), the Harry Mahon Cancer Research Trust, UK, CIHR grant # MOP 44363, and a Canada Chair # 216684 (to NGS). B.M.K. is supported by the Biomedical Research Centre (NIHR), Oxford, UK.

References

Akira S, Uematsu S, Takeuchi O. Pathogen recognition and innate immunity. Cell. 2006; 124:783–801. [PubMed: 16497588]

Bell JK, Mullen GED, Leifer CA, Mazzoni A, Davies DR, Segal DM. Leucine-rich repeats and pathogen recognition in Toll-like receptors. Trends in Immunology. 2003; 24:528–533. [PubMed: 14552836]

Benjamin A. Anticoagulant therapy with coumarin congeners: Action and guidelines. The American Journal of Medicine. 1962; 33:679–691. [PubMed: 14011938]

Blasius AL, Beutler B. Intracellular toll-like receptors. Immunity. 2010; 32:305–315. [PubMed: 20346772]

Brinkmann MM, Spooner E, Hoebe K, Beutler B, Ploegh HL, Kim Y-M. The interaction between the ER membrane protein UNC93B and TLR3, 7, and 9 is crucial for TLR signaling. J Cell Biol. 2007; 177:265–275. [PubMed: 17452530]

Decroly E, Wouters S, Di Bello C, Lazure C, Ruysschaert JM, Seidah NG. Identification of the paired basic convertases implicated in HIV gp160 processing based on in vitro assays and expression in CD4(+) cell lines. J Biol Chem. 1996; 271:30442–30450. [PubMed: 8940009]

Demaison C, Parsley K, Brouns G, Scherr M, Battmer K, Kinnon C, Grez M, Thrasher AJ. High-level transduction and gene expression in hematopoietic repopulating cells using a human imunodeficiency virus type 1-based lentiviral vector containing an internal spleen focus forming virus promoter. Hum Gene Ther. 2002; 13:803–813. [PubMed: 11975847]

Diebold SS, Kaisho T, Hemmi H, Akira S, Reis e Sousa C. Innate antiviral responses by means of TLR7-mediated recognition of single-stranded RNA. Science (New York, NY). 2004; 303:1529–1531.

Diebold SS, Massacrier C, Akira S, Paturel C, Morel Y, Reis e Sousa C. Nucleic acid agonists for Toll-like receptor 7 are defined by the presence of uridine ribonucleotides. European Journal of Immunology. 2006; 36:3256–3267. [PubMed: 17111347]

Ewald SE, Engel A, Lee J, Wang M, Bogyo M, Barton GM. Nucleic acid recognition by Toll-like receptors is coupled to stepwise processing by cathepsins and asparagine endopeptidase. J Exp Med. 2011; 208:643–651. [PubMed: 21402738]

Ewald SE, Lee BL, Lau L, Wickliffe KE, Shi GP, Chapman HA, Barton GM. The ectodomain of Toll-like receptor 9 is cleaved to generate a functional receptor. Nature. 2008; 456:658–662. [PubMed: 18820679]

Fugere M, Limperis PC, Beaulieu-Audy V, Gagnon F, Lavigne P, Klarskov K, Leduc R, Day R. Inhibitory potency and specificity of subtilase-like pro-protein convertase (SPC) prodomains. J Biol Chem. 2002; 277:7648–7656. [PubMed: 11723118]

Govindaraj RG, Manavalan B, Basith S, Choi S. Comparative Analysis of Species-Specific Ligand Recognition in Toll-Like Receptor 8 Signaling: A Hypothesis. PLoS One. 2011; 6

Hallenberger S, Bosch V, Angliker H, Shaw E, Klenk HD, Garten W. Inhibition of furin-mediated cleavage activation of HIV-1 glycoprotein gp160. Nature. 1992; 360:358–361. [PubMed: 1360148]

Heil F, Hemmi H, Hochrein H, Ampenberger F, Kirschning C, Akira S, Lipford G, Wagner H, Bauer S. Species-Specific Recognition of Single-Stranded RNA via Toll-like Receptor 7 and 8. Science. 2004; 303:1526–1529. [PubMed: 14976262]

Honda K, Ohba Y, Yanai H, Negishi H, Mizutani T, Takaoka A, Taya C, Taniguchi T. Spatiotemporal regulation of MyD88-IRF-7 signalling for robust type-I interferon induction. Nature. 2005a; 434:1035–1040. [PubMed: 15815647]

Honda K, Yanai H, Negishi H, Asagiri M, Sato M, Mizutani T, Shimada N, Ohba Y, Takaoka A, Yoshida N, et al. IRF-7 is the master regulator of type-I interferon-dependent immune responses. Nature. 2005b; 434:772–777. [PubMed: 15800576]

Kagan, Jonathan C. Signaling Organelles of the Innate Immune System. Cell. 2012; 151:1168–1178. [PubMed: 23217704]

Kanno A, Yamamoto C, Onji M, Fukui R, Saitoh S, Motoi Y, Shibata T, Matsumoto F, Muta T, Miyake K. Essential role for Toll-like receptor 7 (TLR7)-unique cysteines in an intramolecular disulfide bond, proteolytic cleavage and RNA sensing. Int Immunol. 2013; 25:413–422. [PubMed: 23446849]

Kim YM, Brinkmann MM, Paquet ME, Ploegh HL. UNC93B1 delivers nucleotide-sensing toll-like receptors to endolysosomes. Nature. 2008; 452:234–238. [PubMed: 18305481]

Komiyama T, Coppola JM, Larsen MJ, van Dort ME, Ross BD, Day R, Rehemtulla A, Fuller RS. Inhibition of Furin/Proprotein Convertase-catalyzed Surface and Intracellular Processing by Small Molecules. Journal of Biological Chemistry. 2009; 284:15729–15738. [PubMed: 19332539]

Krug A. Nucleic acid recognition receptors in autoimmunity. Handbook of Experimental Pharmacology. 2008:129–151. [PubMed: 18071658]

Leadbetter EA, Rifkin IR, Hohlbaum AM, Beaudette BC, Shlomchik MJ, Marshak-Rothstein A. Chromatin-IgG complexes activate B cells by dual engagement of IgM and Toll-like receptors. Nature. 2002; 416:603–607. [PubMed: 11948342]

Lee BL, Moon JE, Shu JH, Yuan L, Newman ZR, Schekman R, Barton GM. UNC93B1 mediates differential trafficking of endosomal TLRs. Elife. 2013; 2:e00291. [PubMed: 23426999]

Logeat F, Bessia C, Brou C, LeBail O, Jarriault S, Seidah NG, Israël A. The Notch1 receptor is cleaved constitutively by a furin-like convertase. Proceedings of the National Academy of Sciences of the United States of America. 1998; 95:8108–8112. [PubMed: 9653148]

Malfait A-M, Arner EC, Song R-H, Alston JT, Markosyan S, Staten N, Yang Z, Griggs DW, Tortorella MD. Proprotein convertase activation of aggrecanases in cartilage in situ. Archives of Biochemistry and Biophysics. 2008; 478:43–51. [PubMed: 18671934]

Maschalidi S, Hässler S, Blanc F, Sepulveda FE, Tohme M, Chignard M, van Endert P, Si-Tahar M, Descamps D, Manoury B. Asparagine Endopeptidase Controls Anti-Influenza Virus Immune Responses through TLR7 Activation. PLoS Pathogens. 2012; 8:e1002841. [PubMed: 22916010]

Mohty M, Vialle-Castellano A, Nunes JA, Isnardon D, Olive D, Gaugler W. IFN-alpha skews monocyte differentiation into toll-like receptor 7-expressing dendritic cells with potent functional activities. Journal of Immunology. 2003; 171:3385–3393.

Molloy SS, Bresnahan PA, Leppla SH, Klimpel KR, Thomas G. Human furin is a calcium-dependent serine endoprotease that recognizes the sequence Arg-XX-Arg and efficiently cleaves anthrax toxin protective antigen. Journal of Biological Chemistry. 1992; 267:16396. [PubMed: 1644824]

Nie GY, Li Y, Minoura H, Findlay JK, Salamonsen LA. Specific and transient up-regulation of proprotein convertase 6 at the site of embryo implantation and identification of a unique transcript in mouse uterus during early pregnancy. Biol Reprod. 2003; 68:439–447. [PubMed: 12533406]

Nour N, Basak A, Chretien M, Seidah NG. Structure-function analysis of the prosegment of the proprotein convertase PC5A. J Biol Chem. 2003; 278:2886–2895. [PubMed: 12414802]

Park B, Brinkmann MM, Spooner E, Lee CC, Kim Y-M, Ploegh HL. Proteolytic cleavage in an endolysosomal compartment is required for activation of Toll-like receptor 9. Nature immunology. 2008; 9:1407–1414. [PubMed: 18931679]

Pirher N, Ivicak K, Pohar J, Bencina M, Jerala R. A second binding site for double-stranded RNA in TLR3 and consequences for interferon activation. Nat Struct Mol Biol. 2008; 15:761–763. [PubMed: 18568036]

Rousselet E, Benjannet S, Hamelin J, Canuel M, Seidah NG. The proprotein convertase PC7: unique zymogen activation and trafficking pathways. J Biol Chem. 2011a; 286:2728–2738. [PubMed: 21075846]

Rousselet E, Benjannet S, Marcinkiewicz E, Asselin MC, Lazure C, Seidah NG. The proprotein convertase PC7 enhances the activation of the EGF receptor pathway through processing of the EGF precursor. J Biol Chem. 2011b; 286:9185–9195. [PubMed: 21209099]

Rutz M, Metzger J, Gellert T, Luppa P, Lipford GB, Wagner H, Bauer S. Toll-like receptor 9 binds single-stranded CpG-DNA in a sequence- and pH-dependent manner. European Journal of Immunology. 2004; 34:2541–2550. [PubMed: 15307186]

Salvas A, Benjannet S, Reudelhuber TL, Chretien M, Seidah NG. Evidence for proprotein convertase activity in the endoplasmic reticulum/early Golgi. Febs Lett. 2005; 579:5621–5625. [PubMed: 16213495]

Sasai M, Linehan MM, Iwasaki A. Bifurcation of Toll-Like Receptor 9 Signaling by Adaptor Protein 3. Science. 2010; 329:1530–1534. [PubMed: 20847273]

Seidah NG, Mayer G, Zaid A, Rousselet E, Nassoury N, Poirier S, Essalmani R, Prat A. The activation and physiological functions of the proprotein convertases. The International Journal of Biochemistry & Cell Biology. 2008; 40:1111–1125. [PubMed: 18343183]

Sepulveda FE, Maschalidi S, Colisson R, Heslop L, Ghirelli C, Sakka E, Lennon-Dumenil AM, Amigorena S, Cabanie L, Manoury B. Critical Role for Asparagine Endopeptidase in Endocytic Toll-like Receptor Signaling in Dendritic Cells. Immunity. 2009; 31:737–748. [PubMed: 19879164]

Shlomchik MJ. Activating systemic autoimmunity: B's, T's, and tolls. Current Opinion in Immunology. 2009; 21:626–633. [PubMed: 19800208]

Tabeta K, Hoebe K, Janssen EM, Du X, Georgel P, Crozat K, Mudd S, Mann N, Sovath S, Goode J, et al. The Unc93b1 mutation 3d disrupts exogenous antigen presentation and signaling via Toll-like receptors 3, 7 and 9. Nat Immunol. 2006; 7:156–164. [PubMed: 16415873]

Takahashi S, Kasai K, Hatsuzawa K, Kitamura N, Misumi Y, Ikehara Y, Murakami K, Nakayama K. A mutation of furin causes the lack of precursor-processing activity in human colon carcinoma LoVo cells. Biochemical and Biophysical Research Communications. 1993; 195:1019–1026. [PubMed: 7690548]

Zarkik S, Decroly E, Wattiez R, Seidah NG, Burny A, Ruysschaert JM. Comparative processing of bovine leukemia virus envelope glycoprotein gp72 by subtilisin/kexin-like mammalian convertases. Febs Lett. 1997; 406:205–210. [PubMed: 9109419]

Zhong M, Munzer JS, Basak A, Benjannet S, Mowla SJ, Decroly E, Chretien M, Seidah NG. The prosegments of furin and PC7 as potent inhibitors of proprotein convertases - In vitro and ex vivo assessment of their efficacy and selectivity. Journal of Biological Chemistry. 1999; 274:33913–33920. [PubMed: 10567353]

Europe PMC Funders Author Manuscripts

Highlights

- Human TLR7 is cleaved and accumulates in endosomes independently of low pH
- Calcium-dependent furin-like proprotein convertases (PCs) process TLR7
- Inhibition or knockdown of furin-like PCs reduces responsiveness to TLR7 agonists
- Mutating a furin-like PC recognition site in TLR7 reduces receptor processing

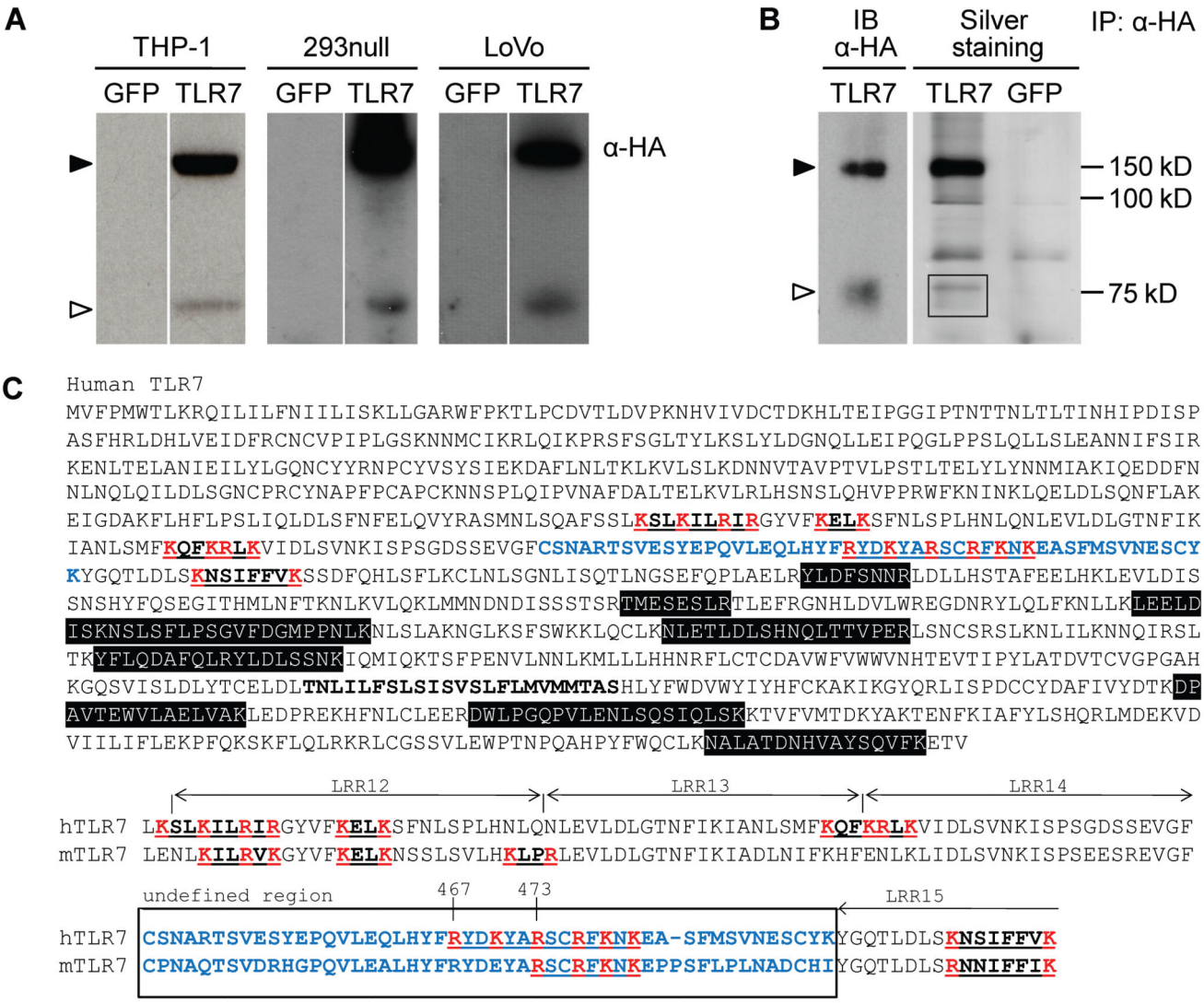

Figure 1. A truncated C-terminal Fragment of TLR7 is Present in Different Human Cell Lines

(A) HA-tagged proteins from THP-, 293null- or LoVo-TLR7 cell lysates were analyzed by Western blot with anti-HA. Representative of more than three independent experiments. (B) Comparison of Western blot and silver staining of proteins immunoprecipitated with anti-HA from THP-TLR7 or THP-GFP treated with PMA for 24 hrs. Box indicates polypeptides analyzed by nano LC-ESIMS/MS tandem mass spectrometry. MS analysis was performed once. (C) Top, hTLR7 sequence, with peptides identified by MS analysis highlighted in black. The undefined region predicted by (Bell et al., 2003) is shown in blue. Potential furin-like PC recognition sites are underlined. Arginine and Lysine residues within those sites are shown in red. Bottom, alignment of the potential PC recognition sites close to the undefined region within the hTLR7 and mTLR7 sequences. Full-length and truncated TLR7 are shown by filled and open arrowheads respectively.

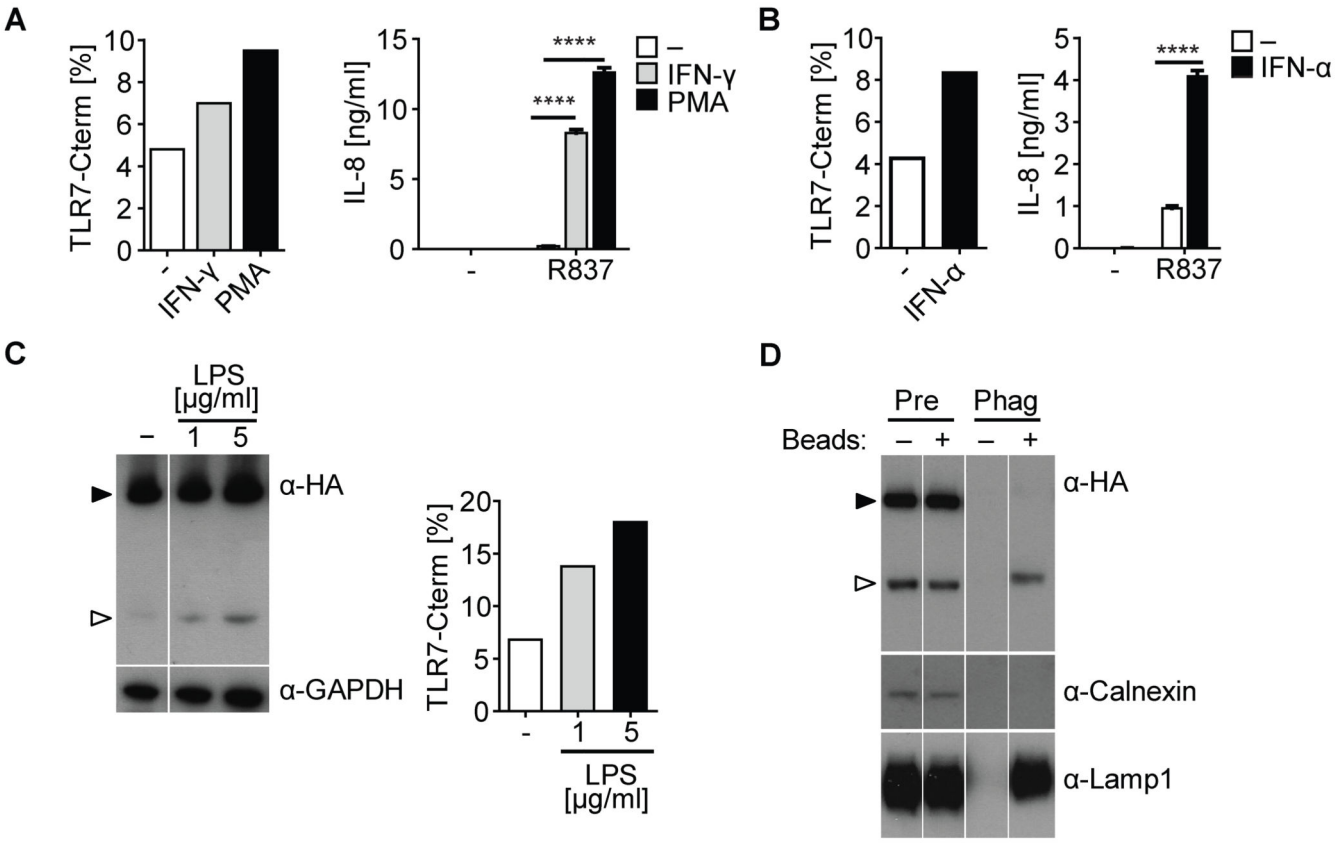

Figure 2. Pro-inflammatory Stimuli Enhance TLR7 Processing and Responses to TLR7 agonists

(A - C) Western blot analysis of cell lysates from THP-TLR7 treated for 24 hrs with 10 nM PMA, 200 U/ml IFN-γ (A), 1000 U/ml IFN-α (B), or with LPS (C). Intensity of truncated TLR7 band is expressed as percentage of the truncated + full-length TLR7 bands. (A and B) THP-TLR7 were differentiated with PMA, IFN-γ, or IFN-α as above, and then stimulated with R837 for another 24 hrs. Values are mean ± S.D. of triplicates. ****, $p < 0.0001$ versus control by Student's t test. (D) Phagosomes were isolated from THP-TLR7 fed with or without latex beads in the presence of R837. Lysates of pre-gradient (Pre) controls or phagosome (Phag) were analyzed by Western blot. Full-length and truncated TLR7 are shown by filled and open arrowheads respectively. Representative of at least three independent experiments (A - D). See also Figure S1.

Europe PMC Funders Author Manuscripts

Europe PMC Funders Author Manuscripts

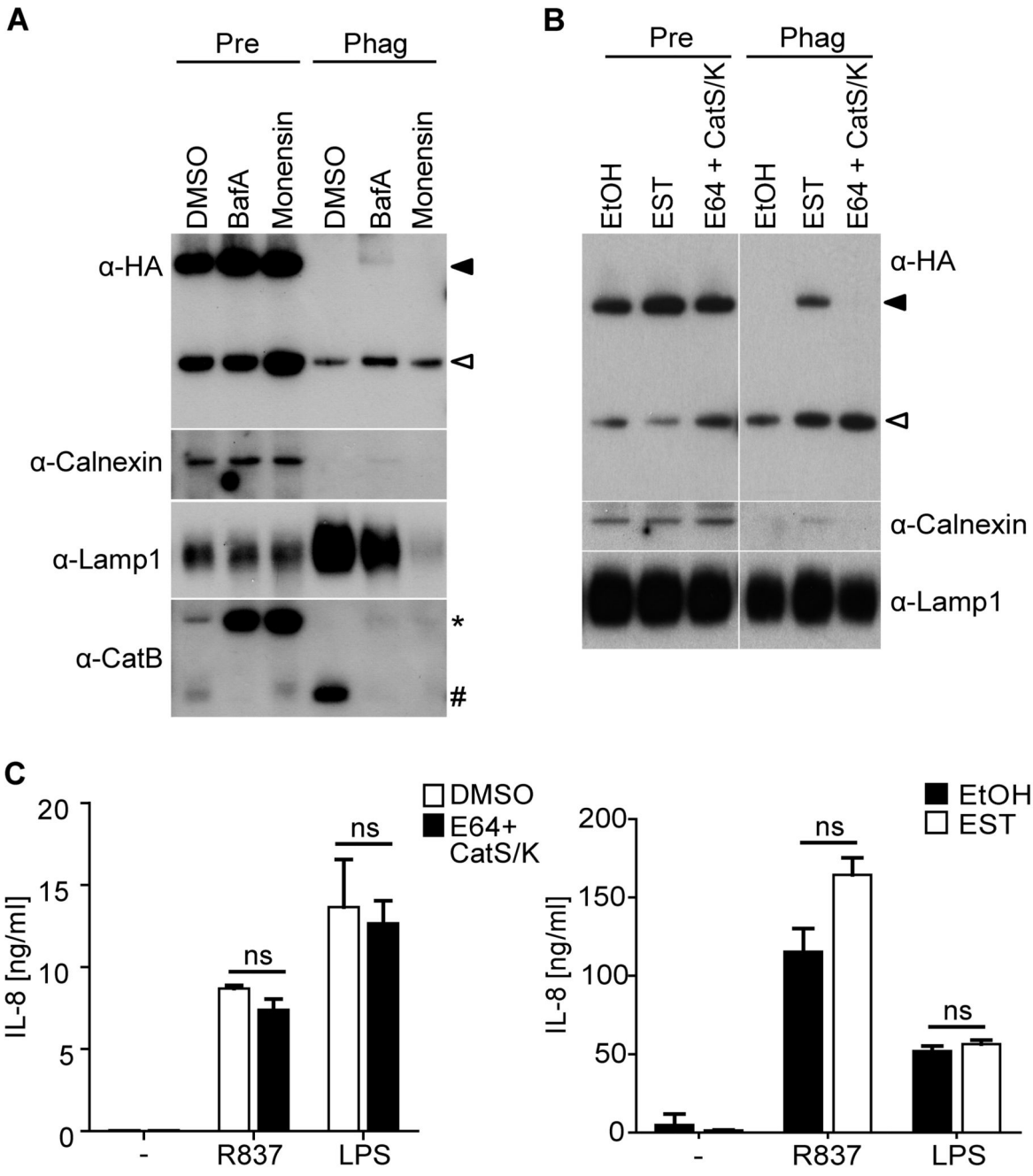

Figure 3. Inhibition of Acidification Does Not Affect the Generation of Truncated TLR7 and its Accumulation in Phagosomes

(A) Western blot analysis of lysates of pre-gradient controls (Pre) or phagosome (Phag) fractions probed with antibodies with the indicated specificity. PMA-differentiated THP-TLR7 cells were treated with indicated inhibitors for 12 hrs before feeding with latex beads in the presence of inhibitors and R837 for 6 hrs. (B) PMA differentiated THP-TLR7 were treated with indicated inhibitors (E64 [20 μM], CatS [2 nM], CatK [1.5 μM], EST [20 μM]) or carrier (ethanol; EtOH) for 24 hrs. Phagosomes were isolated and analyzed as described above. (C) PMA-differentiated THP-TLR7 cells were treated with the indicated inhibitors

for 24 hrs, and then stimulated with R837 or LPS in the presence of inhibitors for another 24 hrs. IL-8 accumulation in culture supernatants was measured by ELISA. Values are mean ± S.D. of triplicates. ns = non significant versus control by Student's t test. Full-length and truncated TLR7 are shown by filled and open arrowheads respectively. * indicates immature pro-CatB and # indicates mature CatB. Representative of at least three independent experiments (A - C). See also Figure S2.

Europe PMC Funders Author Manuscripts

Europe PMC Funders Author Manuscripts

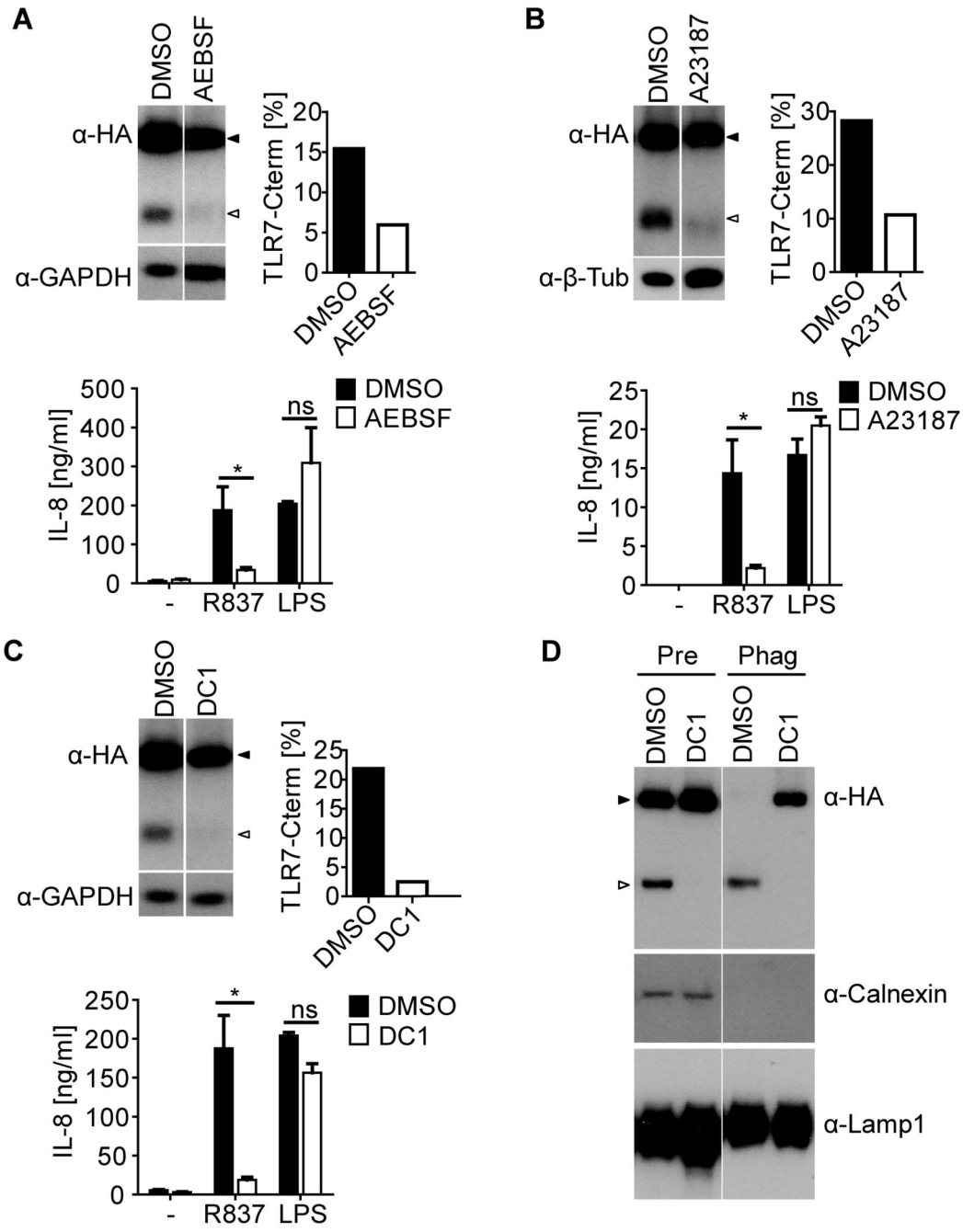

Figure 4. Calcium Dependent Serine-proteases Mediate TLR7 Processing

(A - C) Western blot analysis of cell lysates of PMA differentiated THP-TLR7 treated with AEBSF (0.25 mM) (A), EDTA (0.5 mM) + A23187 (0.5 μM) (B), or DC1 (60 μM) (C) for 24 hrs. Membranes were probed with the indicated antibodies. Bands intensity is expressed as percentage of total TLR7. For cytokine analysis, cells were treated as described above, and then stimulated with R837 or LPS in the presence of inhibitors for another 24 hrs and IL-8 in culture supernatants was measured by ELISA. Values are mean ± S.D. of triplicates. ns = non significant; *, $p < 0.05$ versus control by Student's t test. (D) Western blot analysis

of lysates of pre-gradient controls (Pre) or phagosome fractions (Phag) probed with antibodies specific for the indicated proteins. PMA differentiated THP-TLR7 cells were treated with inhibitors 24 hrs prior to incubation with latex beads in the presence of R837. Full-length and truncated TLR7 are shown by filled and open arrowheads respectively. Representative of at least three independent experiments (A - D). See also Figure S3.

Europe PMC Funders Author Manuscripts

Europe PMC Funders Author Manuscripts

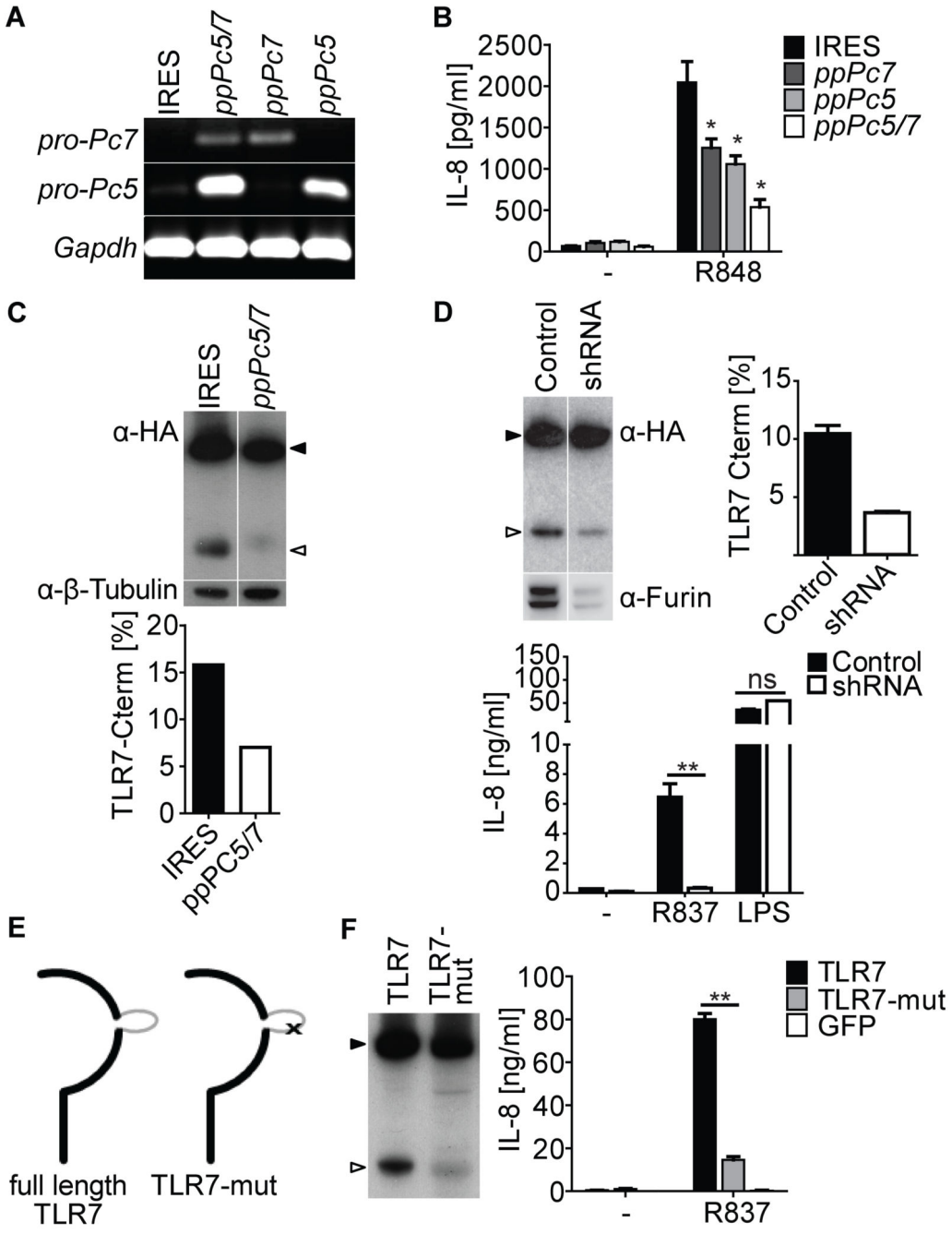

Figure 5. Furin, PC5/6 and PC7 can mediate TLR7 Processing

(A-C) LoVo-TLR7 cells stably expressing IRES control plasmid, or inhibitory preprosegments ppPC7, ppPC5 or ppPC7 and ppPC5 together. (A) Semi-quantitative RT-PCR showing expression of preprosegments. (B) IL-8 in supernatants of LoVo-TLR7 expressing the indicated preprosegments and stimulated for 24 hrs with R848. (C) Western blots of cell lysates of LoVo-TLR7 expressing ppPC5 and ppPC7 and stained for HA. Bands intensity is expressed as percentage of total TLR7. (D) Western blot of cell lysates of THP-TLR7 expressing shRNA against furin or non-target controls stained for HA and furin (top

panel). Bands intensity is expressed as percentage of total TLR7 (top right panel). IL-8 in supernatant of the same cells stimulated for 24 hrs with R837 (1 μg/ml) or LPS (0.1 μg/ml) (bottom panel). (E) Schematic depiction of TLR7 and TLR7-mut. The flexible loop is depicted in gray. 'x' indicates the mutation inserted within the flexible loop. (F) Cell lysates of PMA differentiated THP-1 expressing indicated constructs were analyzed by staining with anti-HA. IL-8 accumulation in culture supernatants of indicated cell lines was monitored by ELISA after 24hrs of stimulation with R837 (10 μg/ml). All IL-8 histograms show mean ± SD (n = 3). ns, non-significant; *, $p < 0.05$; **, $p < 0.01$ by Student's t test versus control. Full-length and truncated TLR7 are shown by filled and open arrowheads respectively. Representative of either two (A) or at least three independent experiments (B - D, F). See also Figure S4.

Europe PMC Funders Author Manuscripts

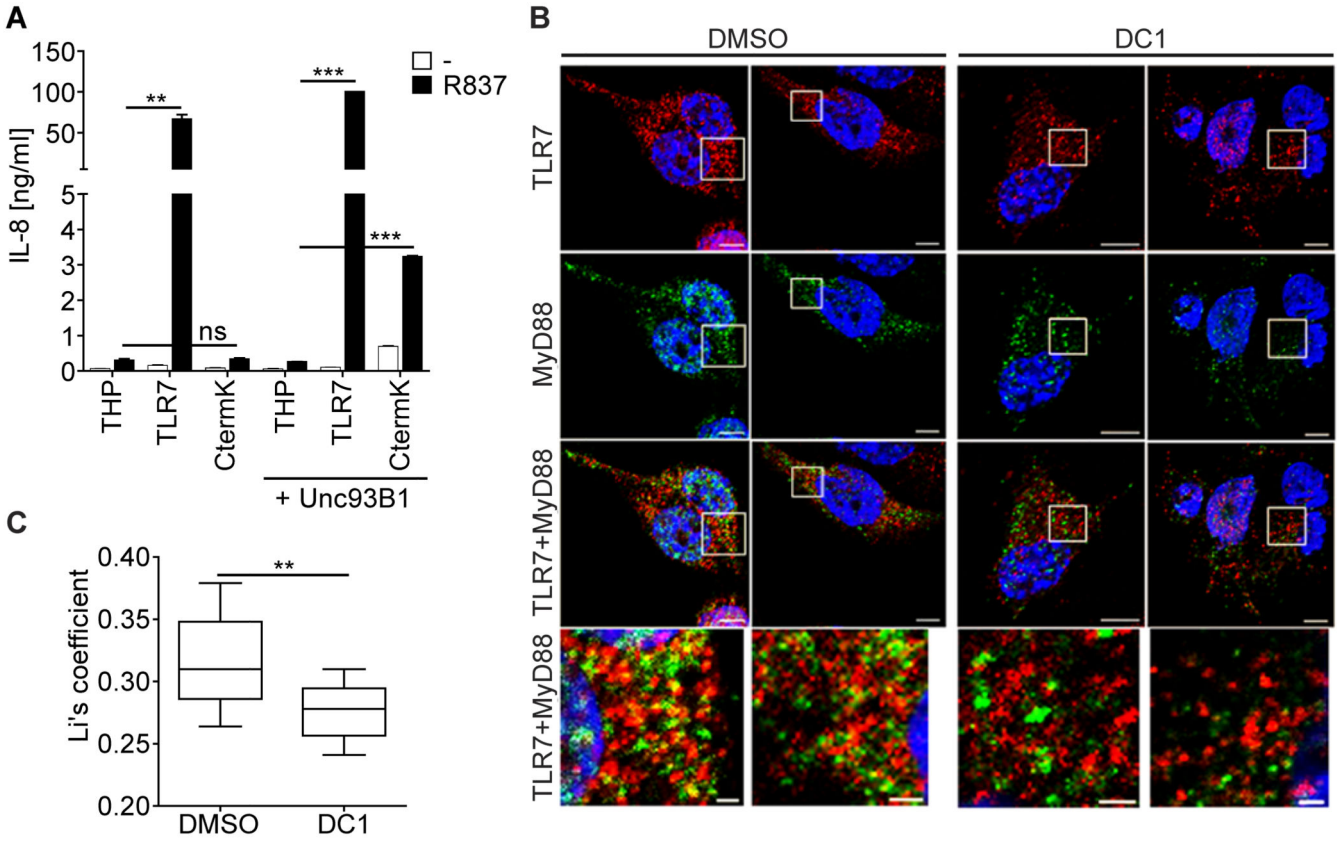

Figure 6. The Truncated version of TLR7 is Signaling Competent.

(A) IL-8 secretion from THP-1 cells expressing the indicated constructs stimulated with R837 for 24 hrs was measured using an ELISA. Values are mean ± S.D. (n=3). (B, C) THP-1 cells expressing HA-tagged TLR7 and FLAG-tagged MyD88 were PMA differentiated for 24 hrs in the presence of DMSO or DC1 (70 μm), and then stimulated for 3 hrs with 5 μg/ml R837. Cells were then fixed and stained with anti-HA (shown in red) and anti-FLAG (shown in green). Confocal pictures were taken. Bars represent 5 μm (top three panels) and 1 μm (bottom panel). (C) Li´s coefficient of ≥ 10 cells per treatment was calculated to quantify the degree of co-localization of MyD88 and TLR7. Data obtained is represented as a box and whisker plot. Stats versus control (Student's t test): **, $p < 0.01$; ***, $p < 0.001$. Representative of three independent experiments (A - C). See also Figure S5.

Europe PMC Funders Author Manuscripts

Europe PMC Funders Author Manuscripts

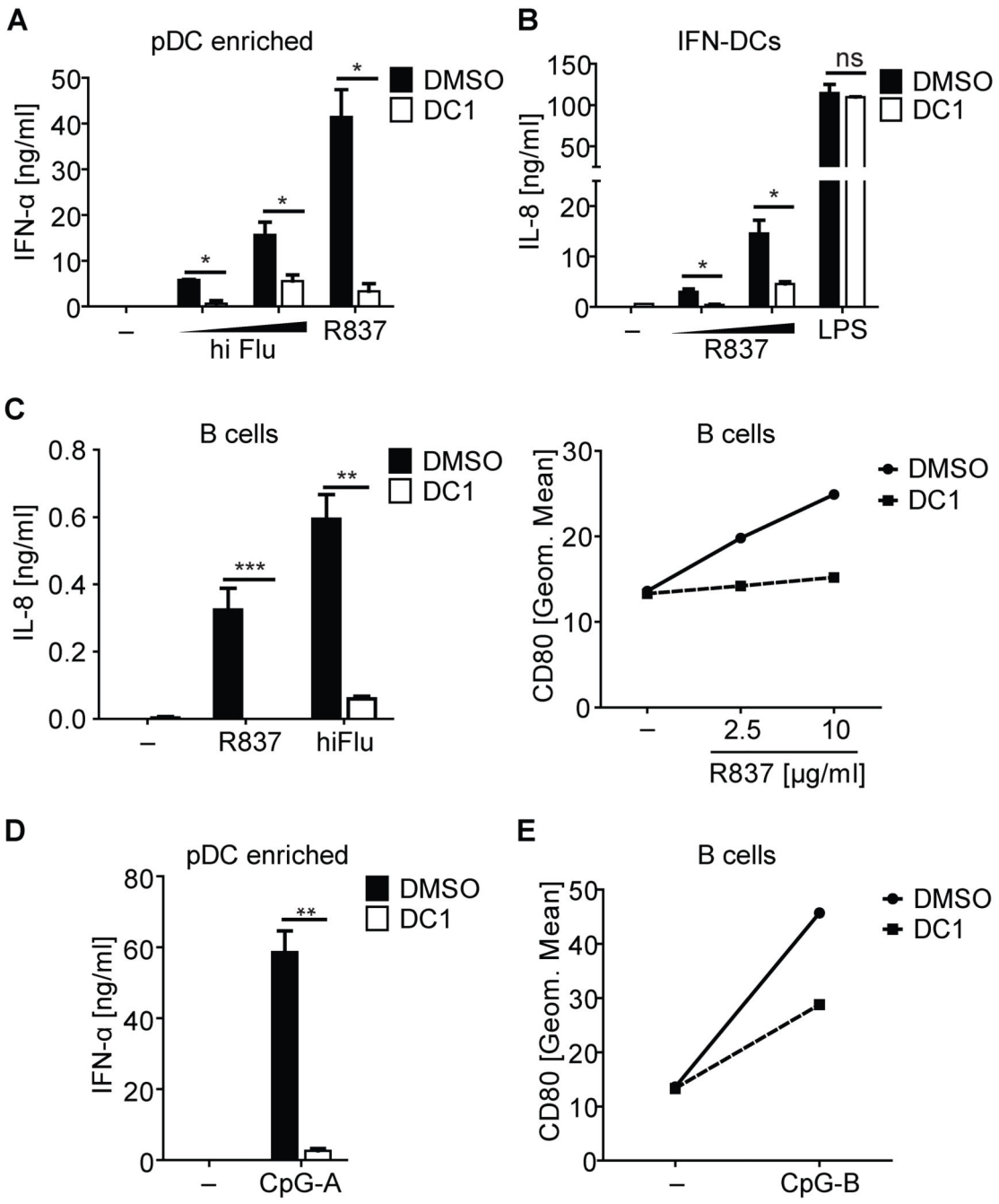

Figure 7. Pharmacological Inhibition of furin-like PCs in pDCs and B cells Reduces Responses to TLR7 and 9 agonists

(A) Human pDC fractions were treated with DMSO or DC1 (70 μM) for 24 hrs, and then stimulated with R837 (1 μg/ml) or hiFlu (equivalent to MOIs of 0.5 or 1) overnight. IFN-α in supernatants was measured by ELISA. Histograms show mean ± SD (n = 2). (B) Human IFN-DCs were treated with DC1 (30 μm) for 24 hrs, and then stimulated with R837 (2.5 or 5 μg/ml) or LPS (0.5 μg/ml) for 36 hrs. Supernatants were harvested and IL-8 content was measured. Histograms show mean ± SD (n = 3). (C) Human blood B cells were treated with DMSO or DC1 (70 μM) for 24 hrs, and then stimulated with R837 (10 μg/ml) or hiFlu

(equivalent to MOI of 1.6) for another 24 hrs. IL-8 in supernatants was measured by ELISA (left panel) and upregulation of CD80 was analyzed by FACS (right panel). Values are mean ± S.D. of triplicates. (D) Human pDC fractions were treated with DMSO or DC1 (70 μM) for 24 hrs, and then stimulated with CpG-A (5 μg/ml) overnight. IFN-α secretion was measured by ELISA. Values are mean ± S.D. of duplicates. (E) Human blood B cells were treated with DMSO or DC1 (70 μM) for 24 hrs, and then stimulated with anti-Fab alone or with anti-Fab ± CpG-B (5 μM) for 24 hrs. Upregulation of cell surface expressed CD80 was analyzed by flow cytometry. ns = non significant; *, $p < 0.05$; **, $p < 0.01$; ***, $p < 0.001$ by Student's t test versus control. Representative of either at least three (A, B) or two (C - E) independent experiments. See also Figure S6.

Europe PMC Funders Author Manuscripts